Hippocampal synaptic and membrane function in the DBA/2J-mdx mouse model of Duchenne muscular dystrophy

Hippocampal synaptic and membrane function in the DBA/2J-*mdx* mouse model of Duchenne muscular dystrophy

Abbreviated title: Duchenne's associated hippocampal hypoexcitability

Key words: Membrane properties, Duchenne's muscle dystrophy, Hippocampus, Synaptic function, after-hyperpolarization.

Authors: Riccardo Bianchi[1,2], Wouter Eilers[3], Federica Pellati[2], Lorenzo Corsi[2], Helen Foster[3], Keith Foster[3] & Francesco Tamagnini[1]

[1] University of Reading School of Pharmacy, Hopkins Building, Whiteknight Campus, Reading, RG6 6LA, UK.
[2] University of Modena and Reggio Emilia, Department of Life Sciences, Via G. Campi 103-287, 41125 Modena, Italy
[3] University of Reading School of Biological Sciences, Hopkins Building, Whiteknight Campus, Reading, RG6 6LA, UK.

Corresponding author: Dr Francesco Tamagnini
Email: F.Tamagnini@reading.ac.uk
T: +44 (0)118 378 4745

Highlights

- **Duchenne's muscular dystrophy is often associated with mental retardation**
- **The association between dystrophin and excitatory neuronal function in hippocampal physiology is yet largely unexplored**
- **We show that hippocampal function is largely preserved in the dystrophin-lacking DBA/2J-*mdx* mouse model**
- **Medium after-hyperpolarization is increased in the DBA/2J-*mdx* mouse model**

Abstract

Dystrophin deficiency is associated with alterations in cell physiology. The functional consequences of dystrophin deficiency are particularly severe for muscle physiology, as observed in Duchenne muscle dystrophy (DMD). DMD is caused by the absence of a 427 kDa isoform of dystrophin. However, in addition to muscular dystrophy symptoms, DMD is frequently associated with memory and attention deficits and epilepsy. While this may be associated with a role for dystrophin in neuronal physiology, it is not clear what neuronal alterations are linked with DMD. Our work shows that CA1 pyramidal neurons from DBA/2J-*mdx* mice have increased afterhyperpolarization compared to WT controls. All the other electrotonic and electrogenic membrane properties were unaffected by this genotype. Finally, basal synaptic transmission, short-term and long-term synaptic plasticity at Schaffer collateral to CA1 glutamatergic synapses were unchanged between *mdx* and WT controls. These data show that the excitatory component of hippocampal activity is largely preserved in DBA/2J-*mdx* mice. Further studies, extending the investigation to the inhibitory GABAergic function, may provide a more complete picture of the functional, network alterations underlying impaired cognition in DMD. In addition, the investigation of changes in neuronal single conductance biophysical properties associated with this genotype, is required to identify the functional alterations associated with dystrophin deficiency and clarify its role in neuronal function.

Introduction

The 427 kDa isoform of dystrophin (Dp427) [1], is present in healthy striated/smooth muscle and neurons, particularly in the hippocampus, prefrontal cortex and cerebellum [2,3]. The lack of dystrophin causes Duchenne muscular dystrophy (DMD) which involves progressive wasting of skeletal muscle and the replacement of muscle tissue with connective and adipose tissue, as well as the development of dilated cardiomyopathy in later stages of the disease [4,5]. In addition, DMD has been associated with altered brain function, including attention deficits, memory impairments and increased risk of seizures, which suggests a role for dystrophin in brain function[6]. In the brain, neurons expressing the Dp427 isoform include cerebellar Purkinje cells, hippocampal and cortical pyramidal cells and cells in the amygdala[7-10]; other brain isoforms are Dp140 and the Dp71 [11,12].

The Dp427 isoform is highly localized in synaptic spines and post-synaptic densities (PSD), where it associates with a dystrophin-associated protein complex (DAPC) which spans the cell membrane and links the actin cytoskeleton with the extracellular matrix [13]. Both spines and PSDs have a critical role for neurotransmission and synaptic plasticity, which underlie cognitive functions, including memory and learning[14]. The cognitive impairment associated with DMD has been linked to the effects of the lack of dystrophin in brain structures associated with memory, language and attention, including the hippocampus and the prefrontal cortex[7,15]. In addition, it should be noted that only one third of DMD patients show cognitive impairment[16]. The cognitive impairment can appear, in the absence of dystrophin, even without the muscular dystrophy symptoms, suggesting that the cognitive symptoms are a direct consequence of the lack of protein, rather than an epiphenomenon paralleling and caused by the motor impairment[17]. Finally, the lack of dystrophin has been associated with epilepsy, as the prevalence of epilepsy in DMD patients is significantly higher in comparison to control populations[18-21].

However, it is not clear yet how the lack of the Dp427 isoform of dystrophin may affect the biophysical properties of membrane conductance and synaptic machinery, responsible for neuronal excitability and synaptic transmission and plasticity, respectively. For example, the

84 *mdx* mouse, the most commonly used mouse model for dystrophin deficiency and DMD, which
85 lacks the expression of the Dp427 kDa dystrophin isoform, has been reported to show
86 impaired spatial memory and enhanced long-term potentiation (LTP) of synaptic transmission
87 in the hippocampus[9,22], while other research groups have not observed differences in either
88 spatial learning or hippocampal LTP[23]. Intriguingly, motivational differences between the *mdx*
89 mouse and its wild type control can give conflicting operant conditioning, dependent on the
90 type of behavioural characteristics being assessed[24]. The reasons for all these discrepancies
91 are unclear; however, the absence of a mechanistic pathway leading from the absence of
92 dystrophin to cognitive dysfunction contributes to the lack of consensus on the causal
93 connection between DMD and neuronal function [25]. In addition, such a variety of hippocampal
94 function phenotypes may be associated with the unpredictability of mental retardation onset
95 in people with DMD (only 1/3 of DMD patients show cognitive deficit)[16].
96 GABA-receptor density and clustering on post-synaptic membranes, and GABA dependent
97 inhibitory neurotransmission have been shown to be altered in *mdx* mice. The frequency of
98 GABAergic-dependent spontaneous inhibitory post-synaptic currents (IPSCs) is indeed
99 increased in the amygdala pyramidal neurons of *mdx* mice, revealing a possible effect of this
100 genotype in promoting the hyperexcitability of inhibitory interneurons in this brain area [9].
101 Much less is known about the effect of the loss of dystrophin on basic electrotonic and
102 electrogenic properties of neuronal membranes. In the light of all the above, in this study we
103 investigated the effects of the absence of Dp427 on the excitability of hippocampal CA1
104 pyramidal neurons as well as the functionality of Schaffer Collaterals – CA1 synapses in
105 DBA/2J-*mdx* mice. This mouse line has been generated by backcrossing the more commonly
106 used Bl/10-*mdx* mouse line onto a DBA/2J genetic background which results in a more severe
107 pathology of the muscle (ref 37, Coley et al). Although our study was not designed to determine
108 the effect of genetic background on neuronal parameters, we reasoned that the increased
109 muscle weakness in the DBA/2J-*mdx* mice compared to the Bl/10-*mdx* mice might compound
110 any effects of the lack of dystrophin per se because of additional mobility restrictions in the

mice due to muscle weakness. To the best of our knowledge, no studies have investigated neuronal function in this DMD model.

Materials and methods

Experimental animals

Male DBA/2J-*mdx* mice (The Jackson Laboratory, Bar Harbour, ME USA) and DBA2 wild-type mice (Envigo, UK) were group housed in animal facilities at the University of Reading on a 12:12 hour light/dark cycle with standard chow and water available at libitum. In all experiments, DBA/2J-*mdx* mice were compared against age- and sex-matched wild-type mice. All experiments were carried out at the University of Reading under a United Kingdom Home Office licence in compliance with the Animals (Scientific Procedures) Act 1986.

Preparation of brain slices.

Animals were sacrificed using cervical dislocation in accordance with schedule 1 of the Animals (Scientific Procedures) Act (1986). The brain was rapidly removed and transferred to an ice cold cutting solution consisting of (in mM): 189 Sucrose, 10 D-Glucose, 26 $NaHCO_3$, 3 KCl, 5 $MgSO_4(7\ H_2O)$, 0.1 $CaCl_2$, 1.25 NaH_2PO_4. Three hundred µm coronal sections were cut using a Leica VT1200 microtome and immediately transferred to a holding chamber containing artificial cerebrospinal fluid (aCSF) continuously perfused with carbogen. The composition of the aCSF was as follows (in mM): 124 NaCl, 3 KCl, 24 $NaHCO_3$, 2 $CaCl_2$, 1.25 NaH_2PO_4, 1 $MgSO_4$, 10 D-glucose. The slices were then allowed to recover for 30 min at 37° C and subsequently at room temperature for at least 1 hour prior to transfer into a recording chamber.

Whole cell patch clamp recordings

Slices were transferred to a recording chamber where they were submerged in carbogen-equilibrated aCSF and maintained at a temperature between 33-34 °C. The recording chamber was secured on the stage of an Olympus BX51 upright microscope and individual CA1 pyramidal neurons were visualised using infrared differential interference contrast optics.

Borosilicate glass microelectrodes with a resistance ranging from 3-7 MΩ were pulled, fire-polished and filled with a K-Gluconate based internal solution consisting of (in mM): 120 mM K-gluconate, 10 mM Na2-phosphocreatine, 0.3 mM Na2-GTP, 10 mM HEPES, 4 mM KCl, 4 mM Mg-ATP (pH 7.2, 280-290 mOsm). Following entry into whole cell configuration, a junction potential error of 15 mV arose due to the pairing of the pipette solution with the aCSF, which was corrected for arithmetically during analysis. Signals were recorded using a Multiclamp 700A amplifier, digitised using a Digidata 1550B and stored for future analysis using pClamp 10 software.

All recordings were made from a defined pre-stimulus membrane potential set by injecting a continuous flow of bias current through the recording electrode. This facilitated the analysis of passive neuronal properties and action potential generation from pre-stimulus membrane potentials (V_m) of both -80 and -74 mV. In order to measure neuronal passive membrane properties a 500 ms, -100 pA hyperpolarising current was injected across the membrane from each V_m. The subsequent voltage deflection at the steady state of the hyperpolarisation was used to calculate the input resistance (R_{in}) of the membrane using Ohm's law (V = IR). The extrapolation of a single exponential curve at an infinite time, fitted to the membrane charging response between 10 and 95% of the peak amplitude, was used to calculate the membrane time constant (τ). An approximation of capacitance was measured as the ratio between the τ and R_{in}.

Sag, measured as the difference between the negative peak and the steady state hyperpolarisation, was expressed as a percentage of the peak hyperpolarisation in response to a 500 ms, -100 pA hyperpolarising current injection.

Standard "Zap" protocols were used to measure subthreshold membrane resonance properties. Briefly, the ratio of the Fast-Fourier transform of the voltage response versus the current injection was calculated as a measure of the impedance profile of the pyramidal neurons ($Z = V_{fft}/I_{fft}$). Subsequently, the impedance versus frequency profile was smoothed

with a 35-point moving average function. The maximal impedance (Z max) frequency at which this maximal impedance occurred (Peak frequency), and the quality factor of the resonator (Q) were quantified to facilitate comparisons between the genotypes. The quality factor of the resonator "Q" was calculated as the ratio between the impedance at peak frequency and the impedance at 0.5 Hz [26].

In order to quantify neuronal excitability, a series of incremental 500 ms depolarising square current injections, ranging from 50 to 350 pA, were injected across the membrane. The number of action potentials (AP) generated for each current injection was used as a measure of excitability. The first AP fired in response to a 350 pA depolarising current step was used to compare action potential waveforms between the genotypes. AP threshold was quantified, defined as the voltage at which the rate of rise (dV/dt) surpassed 20 V s^{-1}; the maximal rate of rise (RoR) was also measured for each cell as the highest value of the first derivative of voltage in time, within the AP duration; the AP width was measured at V_m = -15 mV; finally, the AP peak was measured as the V_m at which, following the ascending phase of the AP, dV/dt=0 V*s^{-1}.

For the voltage-clamp experiments, outside-out, somatic, nucleated macropatches were excised as previously described [27]. Pipette capacitance was neutralized and the series resistance was compensated for (10% – 80% correction). VC recordings were made for the quantitative evaluation of outward-going plateau voltage-gated K^+ currents, by applying 30 ms voltage steps, growing in 10 mV increments and starting from a holding voltage of -90mV. Each recorded current amplitude was normalized to the membrane capacitance of the macropatch in order to account for differences in current amplitude arising from different sizes of the macropatch. The specific current (pA/pF) was plotted against the value of the voltage step.

Field excitatory postsynaptic potentials

Following the initial post-slicing recovery period, the slices were then transferred to a recording chamber in which they were submerged and continually perfused with aCSF, pre-equilibrated

with carbogen and maintained at room temperature. Field excitatory postsynaptic potentials (fEPSPs) were elicited by delivering a short pulse of electrical current (0.1 ms) through tungsten bipolar stimulating electrodes. These stimulating electrodes were placed such as to stimulate axons of the Schaffer Collateral (SC) pathway. Borosilicate glass recording microelectrodes with a resistance ranging from 3-5 MΩ were pulled and filled with aCSF. Recorded signals were collected with a Multiclamp 700A amplifier, digitised with a Digidata 1550B and stored for future analysis using pClamp 10 software.

Input-output curves were constructed by incrementally increasing the current passing through the stimulating electrode and recording the evoked response (0 - 300 µA in 50 µA). For the rest of the experiment, the stimulus intensity was then set to induce 50% c.a. of the maximal response.

Short-term plasticity was tested with a paired-pulse profile, consisting in 2 subsequent stimulating pulses, with inter-pulse intervals of increasing value (in ms): 10, 17, 32, 56, 100, 170, 320, 560, and 1000.

After a period of at least 20 minutes recording baseline responses at low frequency (0.033 Hz), induction of LTP was attempted in the SC-CA1 pathway using a theta-patterned (5 Hz) burst stimulation (TBS) protocol. This consisted of 5 bursts of 10 stimuli at 100 Hz applied with an inter-burst interval of 200 ms. This was repeated 4 times with an inter-repeat interval of 20 s. The fEPSPs were then followed for 1 hour before the TBS protocol was delivered to the other pathway and the fEPSPs were followed up for another hour. We have decided to use TBS over other existing LTP-induction protocols, such as high frequency stimulation [14], as TBS mimics the firing patterns observed *in vivo* in rodents performing a task leading to long-term memory encoding [28-30]. In addition, TBS results in the most effective NMDA- and voltage-gated Calcium channel-dependent form of long-lasting LTP [31-34].

Data analysis

Data were analysed using Clampfit 11. Statistical assessments of differences between genotypes were made using unpaired two-tailed students t-tests and two-way analysis of

variance (ANOVA) as appropriate. Figures were prepared with Origin Pro 2018. All results were expressed as mean ± standard error of the mean (SEM). The experimental "n", refers to the number of slices and to the number of cells we have recorded from in the field potential and patch-clamp experiments, respectively.

Results

Most of the studies investigating the functional correlation between the lack of dystrophin and neuronal and brain dysfunction have focused on the alteration of GABAergic neurotransmission. Our study aimed to characterize, in DBA/2J-*mdx* mice, the effects of the lack of dystrophin on the electrogenic and electrotonic membrane properties of CA1 pyramidal neurons (CA1-PCs). In addition, we investigated whether basal synaptic transmission, short-term synaptic plasticity and long-term potentiation were affected in DBA/2J-*mdx* mice. Field potential, extracellular recordings were carried out in 9 m/o mice, while single cell, whole-cell patch-clamp recordings were carried out in 7 m/o mice. At the chosen age the mice show significant muscle atrophy and weakness (data not shown). In addition, we have observed that DBA/2J-*mdx* mice show less rearing activity but no changes in other activity related parameters, when tested in activity cages (unpublished observations). Whether this is due to the significant reduction in muscle strength in these mice, or due to reduced motivation to act or explore is not known. Previous studies have shown that the mdx genotype is associated with cognitive impairment[35]. However, to our knowledge, there are no available data on the memory performance in DBA/2J-mdx mice.

First, we tested the effect of the DBA/2J-*mdx* genotype on synaptic transmission (Figure 1A; two-way ANOVA; source of variability: genotype; F=3.622, P=0.06), short-term plasticity (Figure 1B; two-way ANOVA; source of variability: genotype; F=0.037, P=0.847) and LTP (Figure 1C; unpaired two-tailed t-test; P=0.97). None of these parameters were affected by the DBA/2J-*mdx* genotype.

Synaptic transmission and plasticity are often regarded as the neuronal correlates of cognitive functions, such as memory and learning; hence a change/impairment in these functional

outcomes would be expected to underlie cognitive dysfunction. However, changes in single cell membrane excitability properties are also fundamental functional correlates underlying cognition, even in the absence of synaptic input/output (I/O), (paired-pulse profile) PPP and long-term potentiation (LTP) alterations. For this reason, we measured the electrotonic and electrogenic membrane properties in CA1-PCs from DBA/2J-*mdx* and age-matched WT controls.

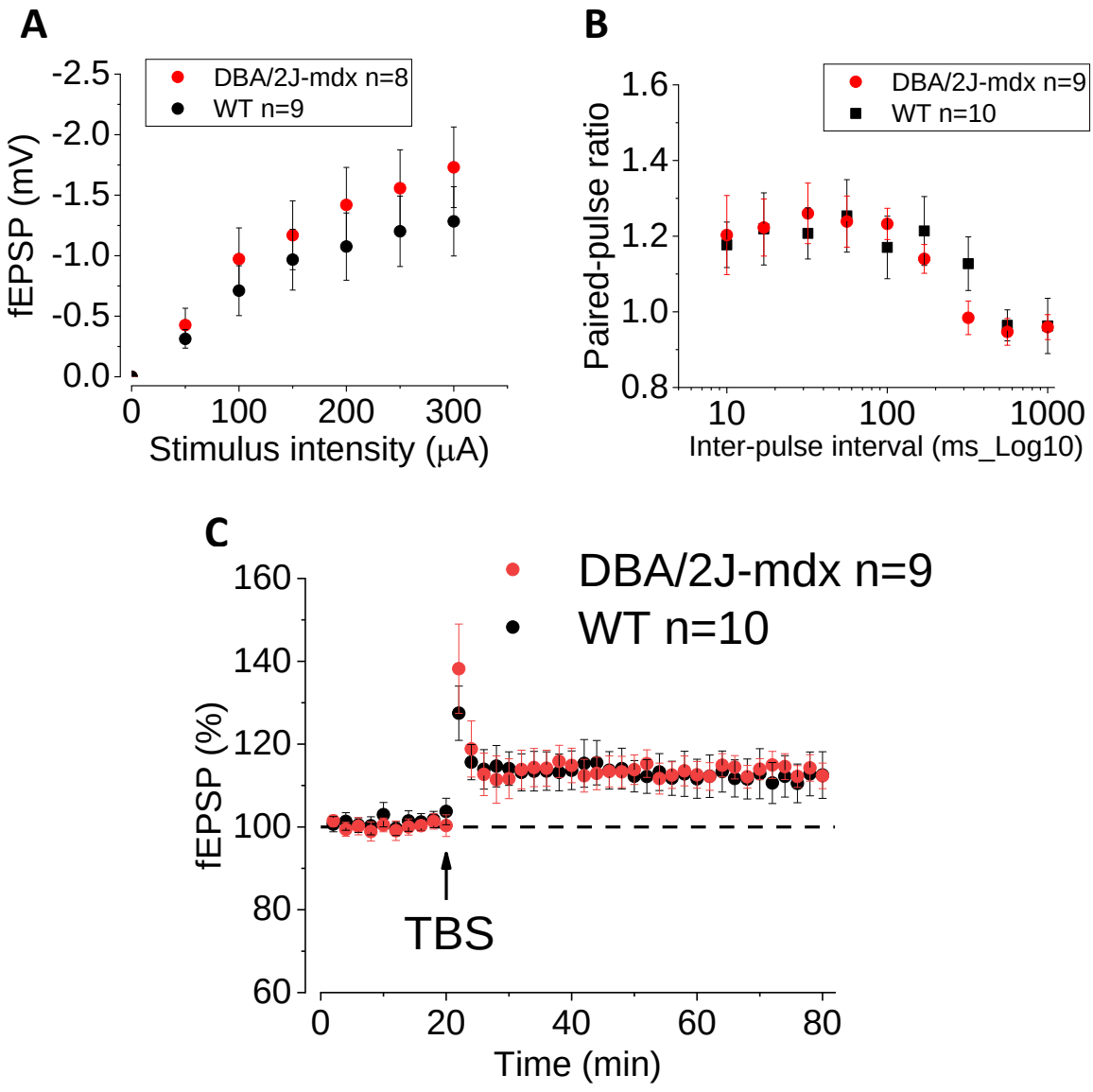

Figure 1. DMD-associated DBA/2J-*mdx* genotype is not associated with impairments of synaptic transmission and plasticity. A. Basal synaptic transmission was measured as the relationship between fEPSP amplitude and stimulus intensities. Input/output curves were built by plotting the amplitude of SC-CA1 fEPSPs amplitude vs stimulus intensity. Two-way ANOVA does not reveal significant differences between genotypes ($F=3.622$ $p=0.06$) nor interactions between genotype and stimulus intensity ($F=0.104$ $p=0.991$). B. Paired pulse ratios of SC-CA1 fEPSPs, tested at increasing inter-pulse intervals, were not different between genotypes (two-way ANOVA; $F=0.037$, $p=0.847$) and no interaction was observed between genotype and ISI (two-way ANOVA; $F=0.499$, $p=0.855$). C. LTP induction in SC-CA1 synapses was not affected by genotype (Unpaired T-Test on the last 10 minutes of follow-up: $p=0.68$). The reported "n" refers to the number of slices.

First, no differences were observed in the resting membrane potential (RMP) between genotypes. To avoid biases arising from cell-to-cell variability in RMP, all the other properties were measured from a pre-stimulus potential of -80 mV, obtained with a constant current

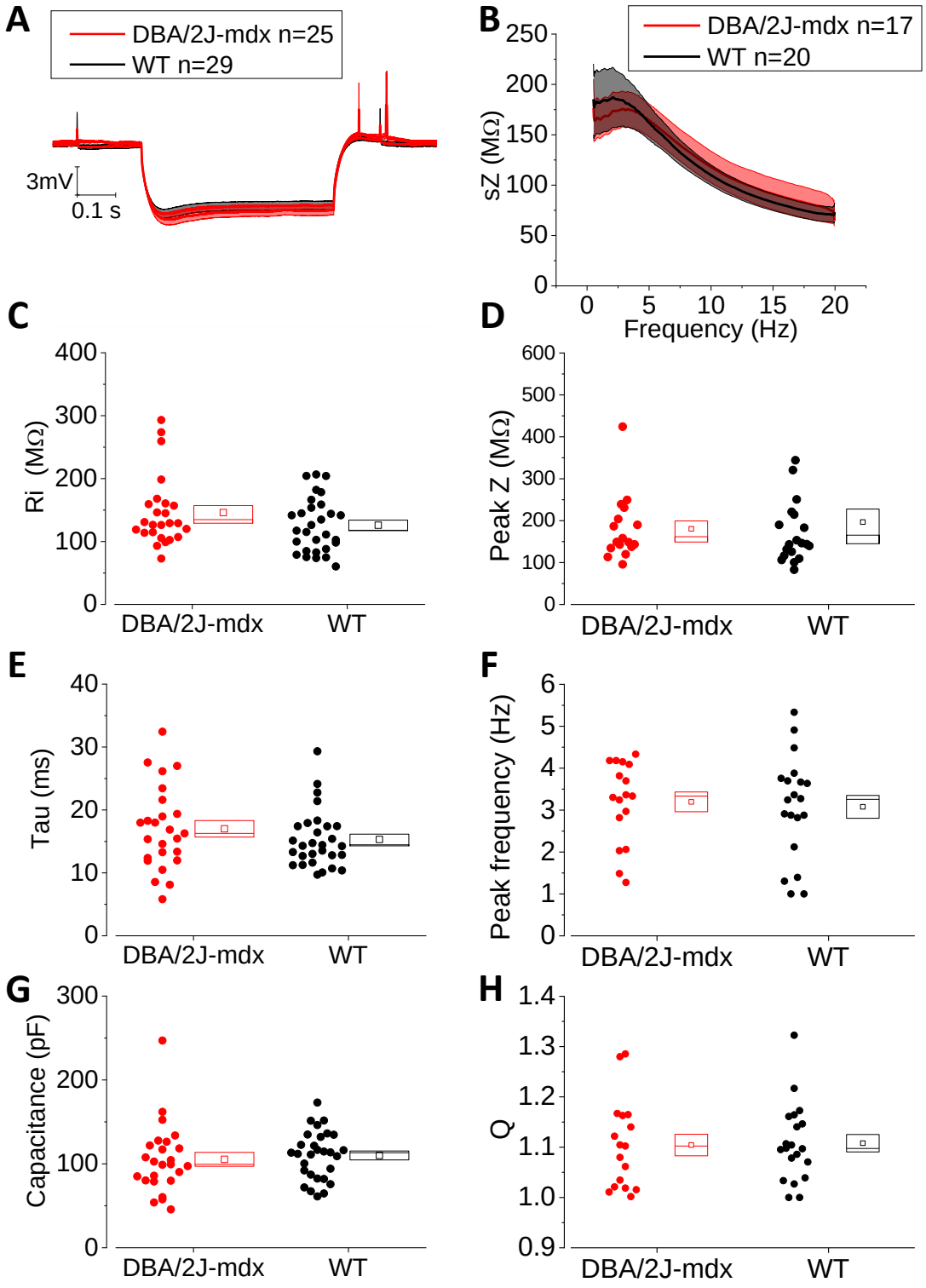

257

Figure 2. DMD-associated DBA/2J-*mdx* genotype does not affect the electrotonic, subthreshold membrane properties in hippocampal CA1-PCs. A. V_m average ± SEM hyperpolarization, upon the injection of a -50 pA, 500 ms current step injection, for each genotype. This approach was used to measure properties like R_{in} (C), Tau (E) and capacitance (G), which were not affected by the *mdx* genotype (unpaired t-test, two tailed). B. Average ± SEM smoothed impedance (sZ), measured upon the injection of a current oscillating at subthreshold values, with frequencies comprised between 0.5 – 20 Hz, is plotted here. Resonance properties were measured between genotypes and no effect was observed between *mdx* mice and WT controls on peak Z (D), peak frequency (F) and quality factor of the resonator Q (H). The reported "n" refers to the number of cells.

injection. No differences were observed in electrotonic passive properties (Figure 1), neither under the injection of a continuous current (Figure 2A, C, E and G) nor the injection of a subthreshold oscillating current, with a frequency linearly increasing between 0.5 Hz and 20 Hz within a 30 s time window (Figure 2B, D, F, and G). This latter approach was used to investigate the effects of DBA/2J-*mdx* genotype on the resonance properties of CA1-PCs, represented as Peak Z, Peak Frequency and quality factor of the resonator – Q, as previously described [36]. Mean, SEM and P values for subthreshold properties in DBA/2J-*mdx* and control mice are reported in Table 1.

Table 1. Subthreshold passive and resonance membrane properties of CA1 pyramidal neurons in hippocampal slices from DBA/2J-*mdx* mice and age-matched WT controls.

	WT n=29 cells		***mdx* n=25 cells**		
Property	**Average**	**SEM**	**Average**	**SEM**	**P**
RMP (mV)	-71.4 (n=39)	2.6	-73.5 (n=33)	3.0	0.6
Rin (MΩ)	126.0	8.0	146.0	11.2	0.1
tau (ms)	15.3	0.8	17.0	1.3	0.3
Capacitance (pF)	110.0	5.3	105.4	8.3	0.6
Peak frequency (Hz)	3.1	0.3	3.2	0.2	0.7
Q	1.11	0.01	1.10	0.02	0.9
Peak Z (MΩ)	196.5	31.1	180.4	18.8	0.7

We tested the firing rate properties of CA1-PCs in DBA/2J-*mdx* and WT controls upon the injection of square current injections of progressively increasing intensity. The average firing rate was not affected by genotype (Figure 3B; two-way ANOVA, source of Variability: genotype, F=0.291, P=0.590).

In addition, the AP waverform properties (Figure 4), namely width (Figure 4C), maximal rate of rise (dV_m/dT) of the AP (RoR) (Figure 4D), peak (Figure 4E) and threshold were not affected by genotype. For averages ± SEM and P values see Table 2.

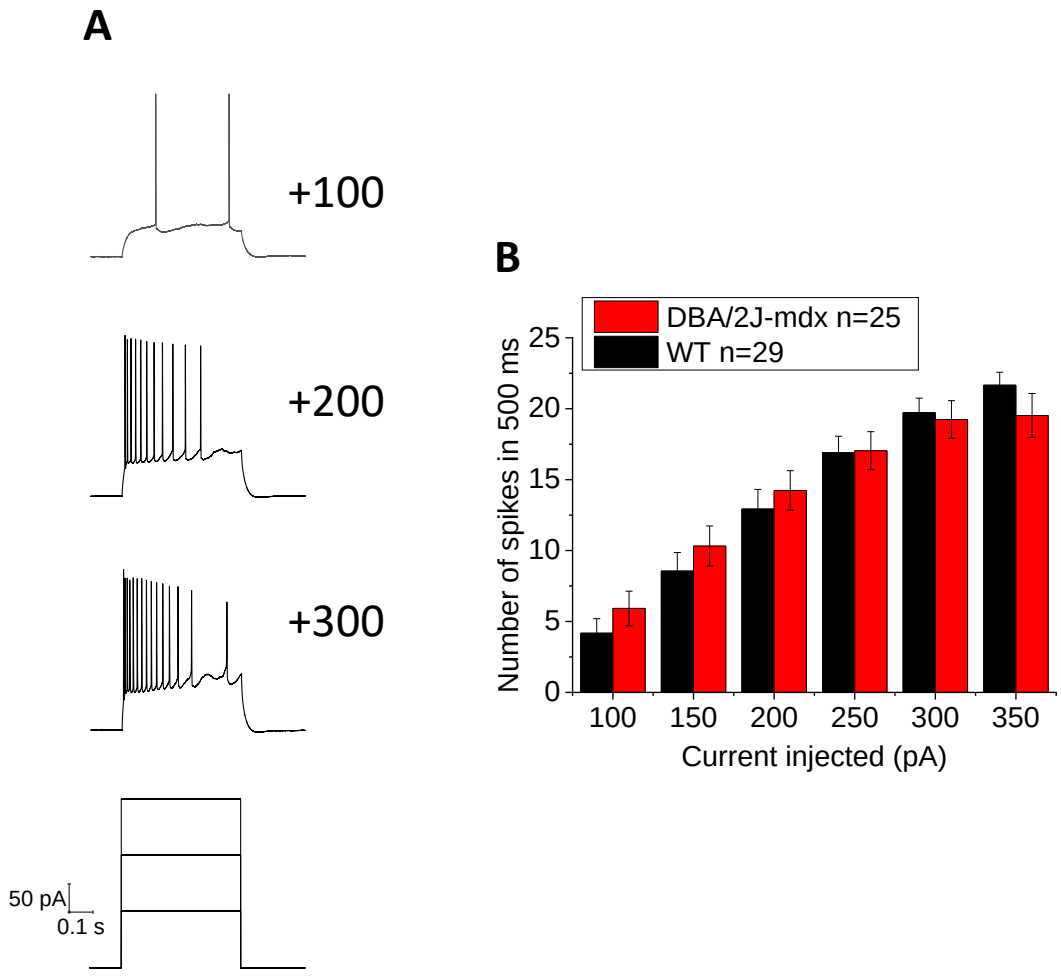

279

Figure 3. DMD-associated DBA/2J-*mdx* genotype does not affect the AP firing rates upon depolarization of the V_m, in hippocampal CA1-PCs. A. Example traces of CA1-PCs firing APs upon the injection of 100 – 200 – 300 pA, 500 ms, depolarizing current steps. B. The number of APs fired at each current intensity (50 – 350 pA, with 50 pA increases), within a 500 ms time window, was plotted as a measure of average firing excitability. No effect of the genotype (two-way ANOVA; F=0.291, p=0.590) nor interaction between genotype and current intensity (two-way ANOVA; F=0.745, p=0.590) was observed on CA1-PCs average firing properties. The reported "n" refers to the number of cells.

280 Post-firing properties, such as the medium component of after-hyperpolarisation (mAHP),
281 were tested to investigate the effect of DBA/2J-*mdx* genotype on the relative refractory
282 period, as an indirect measure of neuronal excitability. mAHPs were evoked by the
283 subsequent application of 5-10-15-20-25, 2 nA-2ms depolarising current steps. The
284 amplitude of the mAHP, comprised of the repolarization of the last evoked AP and the
285 subsequent 500 ms, was measured across number-of-pulses conditions and between
286 genotypes. Figure 5A shows

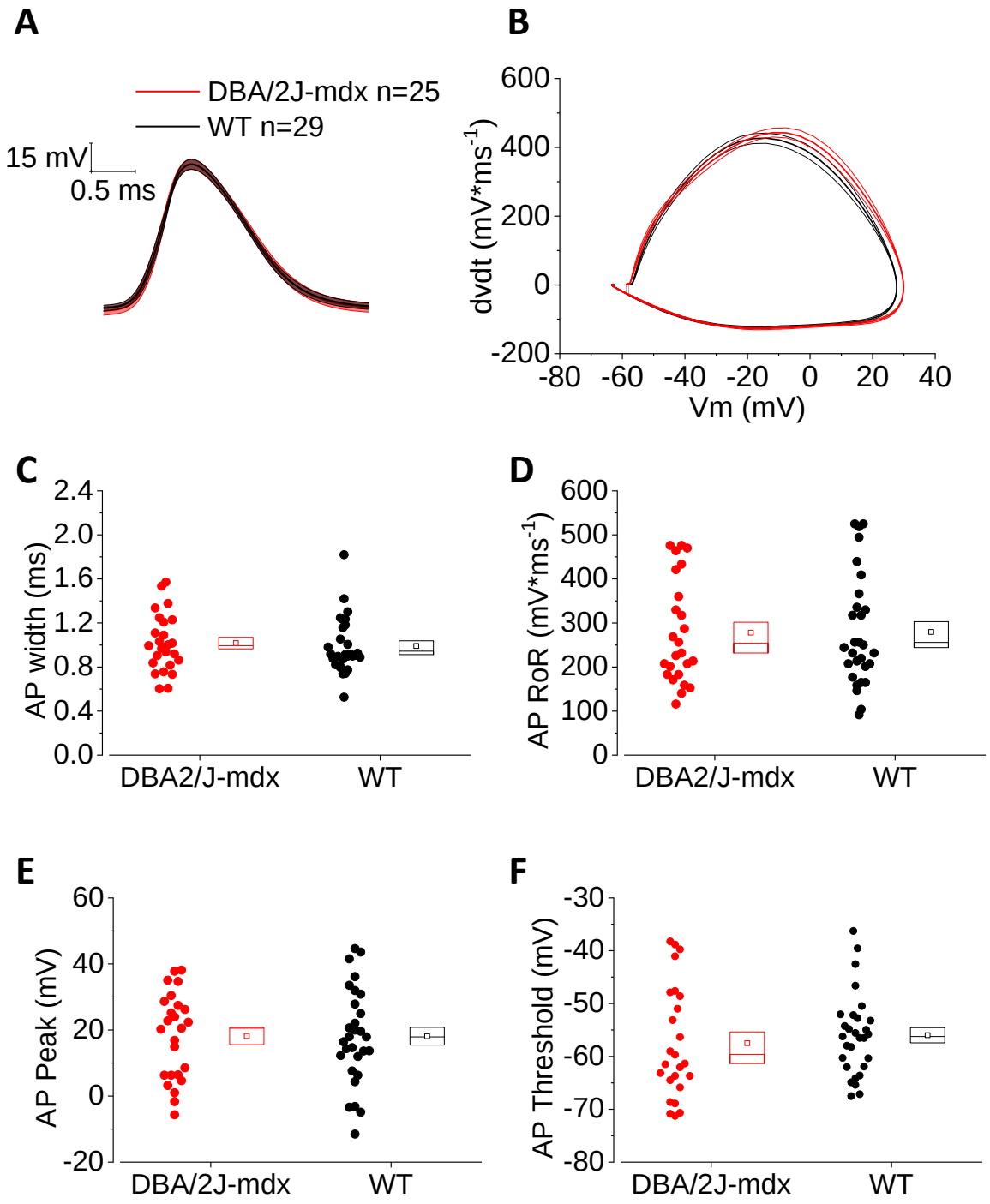

287

Figure 4. DMD-associated DBA/2J-*mdx* genotype does not affect the AP waveform properties in hippocampal CA1-PCs. A. Average ± SEM traces of the first action potential evoked by a 350 pA, 500 ms current step, grouped between genotypes. B. Average ± SEM phase-plots, grouped between genotypes. CA1-PCs action potential waveform properties, such as width (C), maximal rate of rise (D), peak value (E) and threshold (F) are not different between *mdx* and WT controls. The reported "n" refers to the number of cells.

288 the average ± SEM boundaries of the medium and slow components of the AHP evoked by

289 20 pulses, while Figure 5B expands the mAHP component, which is visibly bigger in

DBA/2J- *mdx* CA1-PCs. Two-way ANOVA showed a significant effect of genotype in increasing the mAHP in DBA/2J-*mdx* mice, compared to WT controls (Figure 5C; two-way ANOVA, source of variability: genotype, F=9.687, P=0.002).

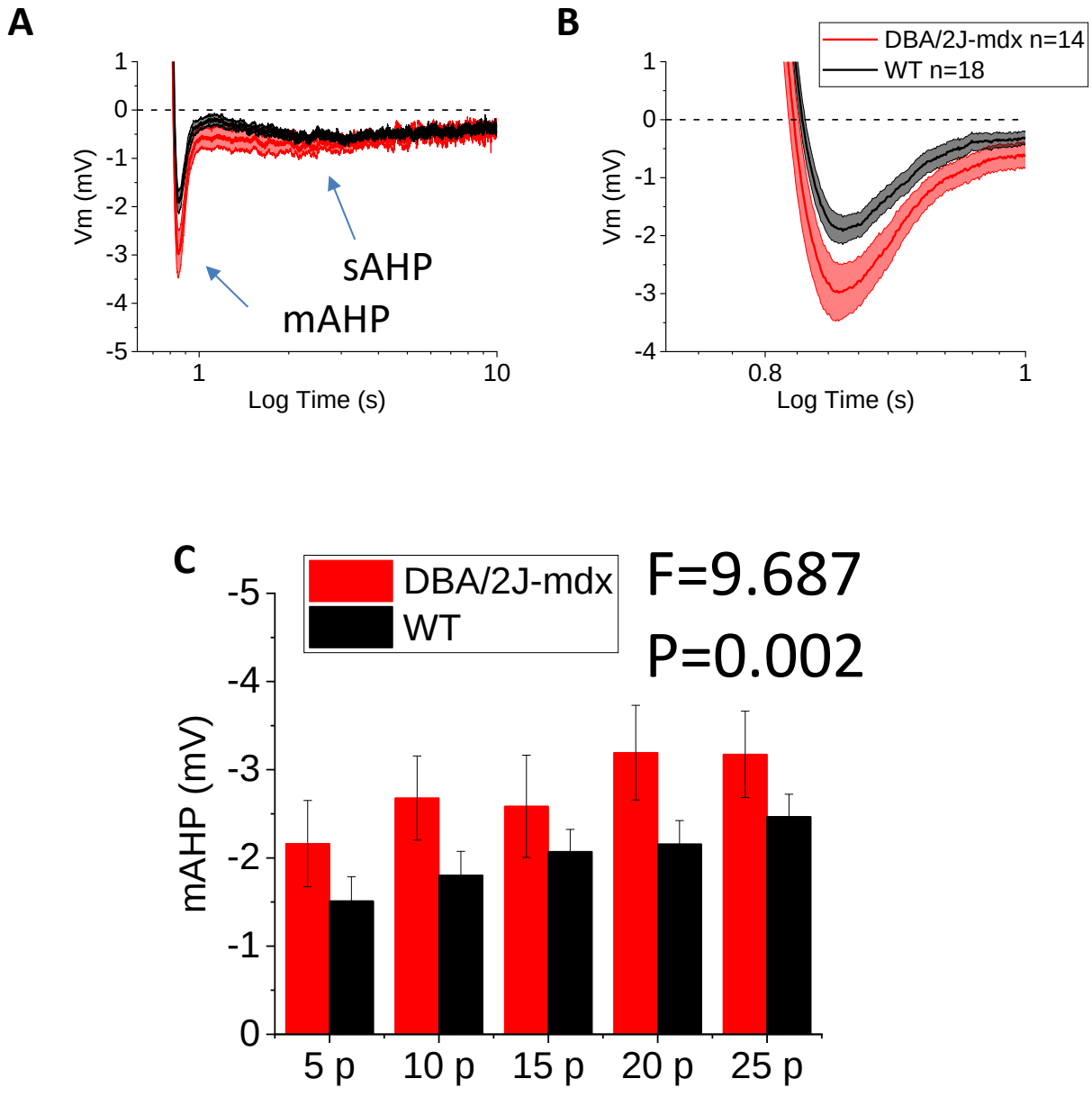

Figure 5. DBA/2J-*mdx* genotype is associated with the increase of the amplitude of post-burst medium but not slow afterhyperpolarizations in hippocampal CA1-PCs. A. Average ± SEM traces of the mAHP evoked by 20 pulses, 2 nA – 2 ms, delivered at 50 Hz, grouped by genotype. An increased mAHP is observed in CA1-PCs from *mdx* mice, but no genotype effect was apparent on slow AHP (B). C. The overall mAHP, evoked by 5-10-15-20-25 2 nA / 2 ms pulses, delivered at 50 Hz, was bigger in *mdx* in comparison to WT controls (two-way ANOVA, F=9.687, p=0.002); however, no interaction was observed between genotype and number of pulses. The reported “n” refers to the number of cells.

Table 2. Action potential properties of CA1 pyramidal neurons in hippocampal slices from DBA/2J-*mdx* mice and age-matched WT controls.

	WT n=29 cells		*mdx* n=25 cells		
Property	**Average**	**SEM**	**Average**	**SEM**	**P**
AP_peak (mV)	18.1	2.7	18.2	2.6	1
AP_width (ms)	0.99	0.05	1.01	0.05	0.7
AP_thres (mV)	-56.0	1.4	-57.5	2.1	0.5
AP_max_dvdt (Vs^{-1})	279.5	23.5	278.1	23.6	1

The generation of mAHP has been ascribed to the gating properties of non-inactivating, voltage-gated K^+ currents, such as I_K [36]. For this reason, we decided to measure the biophysical properties of voltage-gated non-inactivating I_K. Voltage-clamp recordings on nucleated, somatic, outside-out macropatches were performed and cell-to-cell Boltzmann fits were performed to calculate the maximal current density (I_{max}) and the half-activation potential ($V_{1/2}$). However, no significant differences were observed between genotypes for both the I_{max} (Figure 6; DBA/2J-*mdx* I_{max} = 99.7 pA/pF ± 54.4 pA/pF vs WT I_{max} = 136.9 pA/pF ± 62.3 pA/pF; P=0.7) and $V_{1/2}$ (DBA/2J-*mdx* $V_{1/2}$ = -42.6 mV ± 1.9 mV vs WT $V_{1/2}$ = -43.3 mV ± 1.02; P=0.7).

Discussion

We investigated the effects of the lack of dystrophin on both CA1-PCs intrinsic membrane excitability and SC-CA1 glutamatergic synaptic function in a mouse model of muscular dystrophy, the DBA/2J-*mdx*[37,38]. The DBA/2J-*mdx* mouse model, while carrying the same mutation, shows a more severe phenotype, in comparison to *mdx* mice on a Bl/10 genetic background [37,38]. In fact, the DBA/2J background contains genetic modifier loci, which are responsible for the increased severity of symptoms observed in the DBA/2J-mdx mice [39]. To our best knowledge, this is the first-time brain function has been tested in this model. Our main observation was that while synaptic function, electrotonic and firing properties were unaffected by the genotype, the mAHP was bigger in DBA/2J-*mdx* mice than in controls.

We have chosen to carry out the recordings on adult mice, aged 7 and 9-month-old. These ages have been chosen because, while DMD is a disorder mostly affecting people during

development, we were interested to assess the long-term effects of dystrophin deficiency on hippocampal function. In fact, understanding and predicting brain dysfunction associated with DMD, may have a critical role on people's quality of life, should a novel treatment for DMD be developed. While investigating basal synaptic transmission and short-term synaptic plasticity in dystrophin deficient models is novel, LTP has been tested by other groups, showing contrasting results: while some have observed enhanced LTP in dystrophin deficient mice [9,22], others have not found any effect [23]. Our results fit with the latter. Part of the explanation for the discrepancy

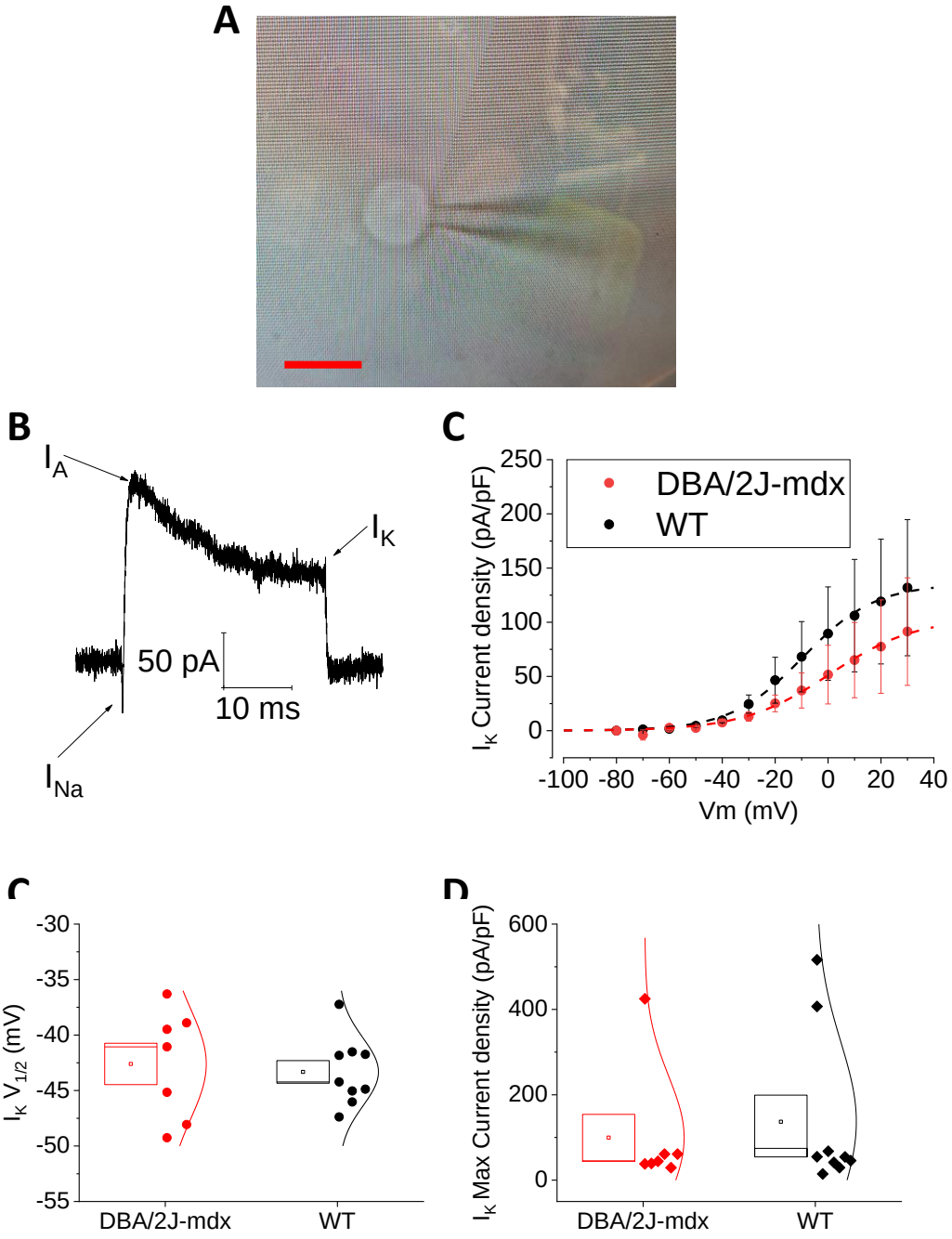

326

Figure 6. The DBA/2J-*mdx* genotype does not affect non-inactivating K^+ currents in CA1-PCs. A. Example of an outside-out nucleated somatic macropatch, pulled from a CA1-PCs at the end of current-clamp recordings. B. Example trace of inward and outward currents evoked by a +30 mV voltage step: because of the fast inactivating kinetics of I_{Na} and I_A, we focused our measures on the inactivating component of voltage-gated outward currents. C. I_K current densities from *mdx* and WT controls plotted versus the intensity of the voltage step. Cell-to-cell fitting of a Boltzmann function was performed to measure somatic I_K maximal current density and $V_{1/2}$. Cell-to-cell analysis of the biophysical properties of CA1-PCs' I_K, revealed no effect of the *mdx* genotype on somatic I_K $V_{1/2}$ (C) and maximal current density (D). Scale bar: 5 µm.

between the results obtained by different groups may be the different conditions used in each study. First, the LTP-inducing stimulation protocol used in each study is different. In fact, both repeated, strong (2x1s at 100Hz every 20 s) and single, weak (1x1s at 30Hz) high frequency stimulation resulted in a genotype-dependent LTP enhancement in *mdx* but not in *mdx*^{3cv} mice [9,22]; however, *in vivo* LTP experiments on *mdx* mice, using 3x1s 100 Hz every 20 s HFS, did not show any genotype-related change in *mdx* mice [23]; finally, our experiments were carried out in DBA/2J-*mdx* mice, using theta-patterned burst (100 Hz) stimulation. Although experiments were carried out in three different DMD mouse models (*mdx, mdx*^{3cv} & DBA/2J-*mdx*) which differ in the severity of the dystrophic pathology, it is currently not possible to conclude whether this influences synaptic plasticity in the brain, because of the use of different protocols by different groups to induce LTP and the fact that dystrophin isoform expression differs between *mdx, mdx*^{3cv} and DBA/2J-*mdx* mice. Given that the muscular pathology of DMD patients is much more severe than that of the *mdx* mouse, and that muscle-secreted and physical activity-induced factors have an influence on brain neurogenesis and synaptic plasticity [40] it would be of interest to determine whether severity of muscle pathology affects synaptic plasticity in DMD mouse models. Our data, obtained from the DBA/2J-*mdx* mouse model, which displays significant muscle atrophy and fibrosis, show no deficit in hippocampal LTP (Figure 1).

Previous work reported that the lack of dystrophin leads to decreased GABAergic neurotransmission [41,42], due to decreased GABA-A clustering on post-synaptic densities [7,43,44]. Reduced GABAergic neurotransmission has been proposed to be the possible mechanism underlying the increased prevalence of epilepsy in boys with DMD [45,46] and enhanced hippocampal LTP in DMD mouse models [9,47]. In addition, the Dp71 isoform-dependent dysregulation of the potassium Kir4.1 channel has been proposed as an alternative/complementary mechanism of action responsible for epilepsy in DMD patients.

However, it is known that altered synaptic function and epileptiform hypersynchronous network activity also rely on the presence of single cell membrane hyperexcitability [27,48-52]. As we did not observe any change in basal synaptic transmission, short- and long-term synaptic

plasticity in DBA/2J-*mdx* mice, we decided to further investigate the effects of lack of dystrophin on the intrinsic physiological properties of the CA1-PC's plasma membrane, as a possible neuronal correlate of DMD-associated brain dysfunction. While electrotonic and firing properties were unchanged between genotypes, the after-hyperpolarization was significantly bigger in DBA/2J-*mdx* mice. mAHP is mediated by voltage-gated K^+ channels (VGKC) [53]. To assess the possible role of VGKC for the alteration of mAHP in *mdx* mice, we performed outside-out nucleated macropatch recordings to assess the biophysical properties of outward voltage-gated currents, as previously reported [27,54]. We did not observe any significant effect of genotype on such current. However, a more detailed investigation of DBA/2J-*mdx*-dependent alterations of biophysical properties is due, as in our native system we could not tease apart the role of each conductance responsible for voltage-gated K^+ currents. In fact, dystrophin deficiency has been linked to an array of changes in membrane K^+ conductances in cardiomyocytes, mediated by different signalling mechanisms. For example, inward rectifier K^+ (K_{ir}) current densities 2.1 were decreased in conditions of dystrophin deficiency [55] but no changes in the protein channel levels were observed, suggesting a change in trafficking rather than expression. In fact, K_{ir} 2.1 is functionally and structurally connected to dystrophin via syntrophin [56] so it has been hypothesized that dystrophin deficiency may result in reduced presence of this conductance on the plasma membrane. However, K_v 2.1 and 1.5 currents, mediating the slow inactivating component of I_k, are also impaired in cardiomyocytes; they are connected to dystrophin via the F-actin and α-actinin-2 network. For this reason, we hypothesize that, in neurons, the lack of dystrophin may result in increased mAHP via syntrophin mediated altered docking of M-current-generating voltage-gated conductances, such as K_v7. In fact, K_v7.x channels have been reported to mediate the mAHP [36].

While previous work has been carried out on the intrinsic excitability of cerebellar Purkinje cells, showing reduced excitability due to hyperpolarized RMP in dystrophin-deficient mice [57], such measures have not been performed before in the hippocampus.

These observations reinforce the idea that dystrophin may play a key role in brain physiology, regulating both motor and cognitive functions. Several lines of evidence show that dystrophin

383 expression is altered in non DMD patients: for example, dystrophin expression is reduced in
384 people with different forms of epilepsy, such as temporal mesial lobe epilepsy [58,59], sclerotic
385 hippocampus [60] and in focal cortical dysplasia [61]. However, while the same phenotype has
386 been observed in the piriform cortex of pilocarpine-induced status epilepticus rats rodent
387 models of epilepsy [62,63], no changes in dystrophin expression have been found in the
388 hippocampus of these animals. On the other hand, dystrophin almost disappeared from the
389 granule cells of the dentate gyrus, following the induction of seizures in mice treated with kainic
390 acid [46]. Such diversity of experimental outcomes somehow reflects the discrepancies
391 observed in the effects of dystrophin deficiency on excitatory synaptic function and it probably
392 reveals the generalized lack of knowledge about the role of this protein on brain physiology.
393 Our results showed increased mAHP in CA1-PCs: this observation may have consequences
394 on network function and cognitive decline observed in people with dystrophin deficiency. In
395 fact, the mAHP corresponds to the refractory period following the AP and has a key role in
396 determining the ability of a single neuron to sustainably fire [36]. An increased mAHP amplitude
397 may result in reduced excitability of the neural network. This, in turn, may account for the
398 cognitive impairment paralleling dystrophin deficiency and be an adaptive mechanism due to
399 increased network excitability. However, the consequences of the increased mAHP in
400 dystrophin deficient mice, both at network and behavioural level, require a more detailed
401 investigation.

402 It should also be highlighted that while our investigation provides important insights into the
403 alterations of hippocampal neuronal function associated with the lack of Dp427 isoforms,
404 cognitive deficits are more significant in DMD patients which lack expression of shorter
405 dystrophin isoforms derived from downstream promoters on the dystrophin gene, in addition
406 to the full length Dp427 isoform [64]. Whether this is because of a specific role for the shorter
407 dystrophin isoforms or whether this is simply due to the further reduction of the presence of
408 C-terminal dystrophin protein domains in the cell is unknown. However, it is currently not
409 possible to study the role of the shorter dystrophin isoforms in isolation due to the mechanism

by which these different isoforms are generated, but it is possible to isolate the role of the Dp427 isoform.

For this reason, we should be cautious in translating these data to all DMD patients. Nonetheless, we believe the results presented here provide insight into the general role of Dp427 in hippocampal function and suggest that the severe muscle dysfunction observed in these mice does not affect most of the CA1 PCs membrane properties.

In addition, the analysis of inhibitory interneurons' intrinsic properties in dystrophin deficient mice is required to better clarify the single cell alterations, which may mechanistically explain the effects of dystrophin deficiency on brain function. Finally, clarifying the role of dystrophin in cognition and the pathological effects of its deficiency in brain function may provide evidence of common pathogenic mechanisms between different disorders resulting in cognitive deficit, including DMD, Alzheimer's disease and epilepsy. This may eventually inform the development of a unified model for the onset different brain diseases resulting in impaired cognition.

Acknowledgements

We thank Erasmus + Traineeship program for funding RB's placement, the University of Reading School of Pharmacy Staff Development and RETF Fund, and Sutura LTD for equipment and consumable expenses.

Author contributions

RB: extracellular recordings and relative data analysis; WE: experimental design, manuscript revision; FP: experimental design and manuscript revision; LC: experimental design and manuscript revision; HF: experimental design and manuscript revision; KF: scientific direction, experimental design and manuscript revision; FT: scientific direction, intracellular recordings, data analysis, experimental design and manuscript preparation.

Competing interests statement

No competing interest

Data availability

The datasets generated during and/or analysed during the current study are available from the corresponding author on reasonable request.

References

1 Hoffman, E. P., Brown, R. H., Jr. & Kunkel, L. M. Dystrophin: the protein product of the Duchenne muscular dystrophy locus. *Cell* **51**, 919-928 (1987).

2 Chamberlain, J. S. *et al.* Expression of the murine Duchenne muscular dystrophy gene in muscle and brain. *Science* **239**, 1416-1418 (1988).

3 Lidov, H. G., Byers, T. J. & Kunkel, L. M. The distribution of dystrophin in the murine central nervous system: an immunocytochemical study. *Neuroscience* **54**, 167-187 (1993).

4 D'Amario, D. *et al.* Dystrophin Cardiomyopathies: Clinical Management, Molecular Pathogenesis and Evolution towards Precision Medicine. *Journal of clinical medicine* **7**, doi:10.3390/jcm7090291 (2018).

5 Yiu, E. M. & Kornberg, A. J. Duchenne muscular dystrophy. *Journal of paediatrics and child health* **51**, 759-764, doi:10.1111/jpc.12868 (2015).

6 Duchenne, G. B. A. Reserches sur la paralysie musculaire pseudeohyper-trofique, ou paralysie myo-sclerosique. *Arch. Gen. Med.* **11**, 5–25, 179–209,305–121, 421–143, 552–188. (1868).

7 Anderson, J. L., Head, S. I., Rae, C. & Morley, J. W. Brain function in Duchenne muscular dystrophy. *Brain : a journal of neurology* **125**, 4-13 (2002).

8 Cyrulnik, S. E. & Hinton, V. J. Duchenne muscular dystrophy: a cerebellar disorder? *Neurosci Biobehav Rev* **32**, 486-496, doi:10.1016/j.neubiorev.2007.09.001 (2008).

9 Vaillend, C., Billard, J. M. & Laroche, S. Impaired long-term spatial and recognition memory and enhanced CA1 hippocampal LTP in the dystrophin-deficient Dmd(mdx) mouse. *Neurobiol Dis* **17**, 10-20, doi:10.1016/j.nbd.2004.05.004 (2004).

10 Doorenweerd, N. *et al.* Timing and localization of human dystrophin isoform expression provide insights into the cognitive phenotype of Duchenne muscular dystrophy. *Scientific reports* **7**, 12575-12575, doi:10.1038/s41598-017-12981-5 (2017).

11 Lidov, H. G., Selig, S. & Kunkel, L. M. Dp140: a novel 140 kDa CNS transcript from the dystrophin locus. *Hum Mol Genet* **4**, 329-335 (1995).

12 de Brouwer, A. P. *et al.* A 3-base pair deletion, c.9711_9713del, in DMD results in intellectual disability without muscular dystrophy. *European journal of human genetics : EJHG* **22**, 480-485, doi:10.1038/ejhg.2013.169 (2014).

13 Kim, T. W., Wu, K., Xu, J. L. & Black, I. B. Detection of dystrophin in the postsynaptic density of rat brain and deficiency in a mouse model of Duchenne muscular dystrophy. *Proc Natl Acad Sci U S A* **89**, 11642-11644 (1992).

14 Bliss, T. V. & Collingridge, G. L. A synaptic model of memory: long-term potentiation in the hippocampus. *Nature* **361**, 31-39, doi:10.1038/361031a0 (1993).

15 Waite, A., Tinsley, C. L., Locke, M. & Blake, D. J. The neurobiology of the dystrophin-associated glycoprotein complex. *Annals of medicine* **41**, 344-359, doi:10.1080/07853890802668522 (2009).
16 Anand, A. *et al.* Dystrophin induced cognitive impairment: mechanisms, models and therapeutic strategies. *Annals of neurosciences* **22**, 108-118, doi:10.5214/ans.0972.7531.221210 (2015).
17 de Brouwer, A. P. M. *et al.* A 3-base pair deletion, c.9711_9713del, in DMD results in intellectual disability without muscular dystrophy. *European journal of human genetics : EJHG* **22**, 480-485, doi:10.1038/ejhg.2013.169 (2014).
18 Goodwin, F., Muntoni, F. & Dubowitz, V. Epilepsy in Duchenne and Becker muscular dystrophies. *Eur J Paediatr Neurol* **1**, 115-119 (1997).
19 Etemadifar, M. & Molaei, S. Epilepsy in Boys with Duchenne Muscular Dystrophy *Journal of Research in Medical Sciences* **3**, 116-119 (2004).
20 Pane, M. *et al.* Duchenne muscular dystrophy and epilepsy. *Neuromuscul Disord* **23**, 313-315, doi:10.1016/j.nmd.2013.01.011 (2013).
21 Hendriksen, R. G. *et al.* A possible role of dystrophin in neuronal excitability: a review of the current literature. *Neurosci Biobehav Rev* **51**, 255-262, doi:10.1016/j.neubiorev.2015.01.023 (2015).
22 Vaillend, C. *et al.* Spatial discrimination learning and CA1 hippocampal synaptic plasticity in mdx and mdx3cv mice lacking dystrophin gene products. *Neuroscience* **86**, 53-66 (1998).
23 Sesay, A. K., Errington, M. L., Levita, L. & Bliss, T. V. Spatial learning and hippocampal long-term potentiation are not impaired in mdx mice. *Neuroscience letters* **211**, 207-210 (1996).
24 Lewon, M. *et al.* Evaluation of the behavioral characteristics of the mdx mouse model of duchenne muscular dystrophy through operant conditioning procedures. *Behavioural processes* **142**, 8-20, doi:10.1016/j.beproc.2017.05.012 (2017).
25 Wikiera, B., Jakubiak, A., Zimowski, J., Noczynska, A. & Smigiel, R. Complex glycerol kinase deficiency - X-linked contiguous gene syndrome involving congenital adrenal hypoplasia, glycerol kinase deficiency, muscular Duchenne dystrophy and intellectual disability (IL1RAPL gene deletion). *Pediatric endocrinology, diabetes, and metabolism* **18**, 153-157 (2012).
26 Vazifehkhah Ghaffari, B., Kouhnavard, M., Aihara, T. & Kitajima, T. Mathematical modeling of subthreshold resonant properties in pyloric dilator neurons. *BioMed research international* **2015**, 135787, doi:10.1155/2015/135787 (2015).
27 Brown, J. T., Chin, J., Leiser, S. C., Pangalos, M. N. & Randall, A. D. Altered intrinsic neuronal excitability and reduced Na+ currents in a mouse model of Alzheimer's disease. *Neurobiology of aging* **32**, 2109 e2101-2114, doi:10.1016/j.neurobiolaging.2011.05.025 (2011).
28 Ranck, J. B., Jr. Studies on single neurons in dorsal hippocampal formation and septum in unrestrained rats. I. Behavioral correlates and firing repertoires. *Experimental neurology* **41**, 461-531 (1973).
29 Otto, T., Eichenbaum, H., Wiener, S. I. & Wible, C. G. Learning-related patterns of CA1 spike trains parallel stimulation parameters optimal for inducing hippocampal long-term potentiation. *Hippocampus* **1**, 181-192, doi:10.1002/hipo.450010206 (1991).
30 Hill, A. J. First occurrence of hippocampal spatial firing in a new environment. *Experimental neurology* **62**, 282-297, doi:https://doi.org/10.1016/0014-4886(78)90058-4 (1978).

31 Grover, L. M. & Teyler, T. J. Two components of long-term potentiation induced by different patterns of afferent activation. *Nature* **347**, 477-479, doi:10.1038/347477a0 (1990).

32 Grover, L. M. & Teyler, T. J. Activation of NMDA receptors in hippocampal area CA1 by low and high frequency orthodromic stimulation and their contribution to induction of long-term potentiation. *Synapse (New York, N.Y.)* **16**, 66-75, doi:10.1002/syn.890160108 (1994).

33 O'Connor, J. J., Rowan, M. J. & Anwyl, R. Long-lasting enhancement of NMDA receptor-mediated synaptic transmission by metabotropic glutamate receptor activation. *Nature* **367**, 557-559, doi:10.1038/367557a0 (1994).

34 O'Leary, D. M. & O'Connor, J. J. Potentiation of synaptic transmission by (S)-3,5-dihydroxy phenylglycine in the rat dentate gyrus in vitro: a role for voltage dependent calcium channels and protein kinase C. *Progress in neuro-psychopharmacology & biological psychiatry* **23**, 133-147 (1999).

35 Comim, C. M. *et al.* Neurocognitive Impairment in mdx Mice. *Molecular Neurobiology* **56**, 7608-7616, doi:10.1007/s12035-019-1573-7 (2019).

36 Gu, N., Vervaeke, K., Hu, H. & Storm, J. F. Kv7/KCNQ/M and HCN/h, but not KCa2/SK channels, contribute to the somatic medium after-hyperpolarization and excitability control in CA1 hippocampal pyramidal cells. *J Physiol* **566**, 689-715, doi:10.1113/jphysiol.2005.086835 (2005).

37 Coley, W. D. *et al.* Effect of genetic background on the dystrophic phenotype in mdx mice. *Hum Mol Genet* **25**, 130-145, doi:10.1093/hmg/ddv460 (2016).

38 Hakim, C. H. *et al.* A Five-Repeat Micro-Dystrophin Gene Ameliorated Dystrophic Phenotype in the Severe DBA/2J-mdx Model of Duchenne Muscular Dystrophy. *Mol Ther Methods Clin Dev* **6**, 216-230, doi:10.1016/j.omtm.2017.06.006 (2017).

39 Coley, W. D. *et al.* Effect of genetic background on the dystrophic phenotype in mdx mice. *Hum Mol Genet* **25**, 130-145, doi:10.1093/hmg/ddv460 (2016).

40 Lourenco, M. V. *et al.* Exercise-linked FNDC5/irisin rescues synaptic plasticity and memory defects in Alzheimer's models. *Nat Med* **25**, 165-175, doi:10.1038/s41591-018-0275-4 (2019).

41 Kueh, S. L., Head, S. I. & Morley, J. W. GABA(A) receptor expression and inhibitory post-synaptic currents in cerebellar Purkinje cells in dystrophin-deficient mdx mice. *Clin Exp Pharmacol Physiol* **35**, 207-210, doi:10.1111/j.1440-1681.2007.04816.x (2008).

42 Nusser, Z., Cull-Candy, S. & Farrant, M. Differences in synaptic GABA(A) receptor number underlie variation in GABA mini amplitude. *Neuron* **19**, 697-709 (1997).

43 Vaillend, C. *et al.* Rescue of a dystrophin-like protein by exon skipping in vivo restores GABAA-receptor clustering in the hippocampus of the mdx mouse. *Mol Ther* **18**, 1683-1688, doi:10.1038/mt.2010.134 (2010).

44 Waite, A., Brown, S. C. & Blake, D. J. The dystrophin-glycoprotein complex in brain development and disease. *Trends Neurosci* **35**, 487-496, doi:10.1016/j.tins.2012.04.004 (2012).

45 Nakao, K., Kito, S., Muro, T., Tomonaga, M. & Mozai, T. Nervous system involvement in progressive muscular dystrophy. *Proc Aust Assoc Neurol* **5**, 557-564 (1968).

46 Knuesel, I., Zuellig, R. A., Schaub, M. C. & Fritschy, J. M. Alterations in dystrophin and utrophin expression parallel the reorganization of GABAergic synapses in a mouse model of temporal lobe epilepsy. *Eur J Neurosci* **13**, 1113-1124 (2001).

47 Vaillend, C., Ungerer, A. & Billard, J. M. Facilitated NMDA receptor-mediated synaptic plasticity in the hippocampal CA1 area of dystrophin-deficient mice.

Synapse **33**, 59-70, doi:10.1002/(sici)1098-2396(199907)33:1<59::aid-syn6>3.0.co;2-k (1999).

48 Palop, J. J. *et al.* Aberrant excitatory neuronal activity and compensatory remodeling of inhibitory hippocampal circuits in mouse models of Alzheimer's disease. *Neuron* **55**, 697-711, doi:10.1016/j.neuron.2007.07.025 (2007).

49 Tamagnini, F. *et al.* Altered intrinsic excitability of hippocampal CA1 pyramidal neurons in aged PDAPP mice. *Frontiers in cellular neuroscience* **9**, 372, doi:10.3389/fncel.2015.00372 (2015).

50 Tamagnini, F., Scullion, S., Brown, J. T. & Randall, A. D. Intrinsic excitability changes induced by acute treatment of hippocampal CA1 pyramidal neurons with exogenous amyloid beta peptide. *Hippocampus* **25**, 786-797, doi:10.1002/hipo.22403 (2015).

51 Kerrigan, T. L. & Randall, A. D. A new player in the "synaptopathy" of Alzheimer's disease - arc/arg 3.1. *Front Neurol* **4**, 9, doi:10.3389/fneur.2013.00009 (2013).

52 Randall, A. D., Witton, J., Booth, C., Hynes-Allen, A. & Brown, J. T. The functional neurophysiology of the amyloid precursor protein (APP) processing pathway. *Neuropharmacology* **59**, 243-267, doi:10.1016/j.neuropharm.2010.02.011 (2010).

53 Gu, N., Vervaeke, K., Hu, H. & Storm, J. F. Kv7/KCNQ/M and HCN/h, but not KCa2/SK channels, contribute to the somatic medium after-hyperpolarization and excitability control in CA1 hippocampal pyramidal cells. *The Journal of physiology* **566**, 689-715, doi:10.1113/jphysiol.2005.086835 (2005).

54 Tamagnini, F. *et al.* Hippocampal neurophysiology is modified by a disease-associated C-terminal fragment of tau protein. *Neurobiology of aging* **60**, 44-56, doi:10.1016/j.neurobiolaging.2017.07.005 (2017).

55 Rubi, L., Koenig, X., Kubista, H., Todt, H. & Hilber, K. Decreased inward rectifier potassium current IK1 in dystrophin-deficient ventricular cardiomyocytes. *Channels (Austin, Tex.)* **11**, 101-108, doi:10.1080/19336950.2016.1228498 (2017).

56 Willis, B. C., Ponce-Balbuena, D. & Jalife, J. Protein assemblies of sodium and inward rectifier potassium channels control cardiac excitability and arrhythmogenesis. *American journal of physiology. Heart and circulatory physiology* **308**, H1463-1473, doi:10.1152/ajpheart.00176.2015 (2015).

57 Snow, W. M., Anderson, J. E. & Fry, M. Regional and genotypic differences in intrinsic electrophysiological properties of cerebellar Purkinje neurons from wild-type and dystrophin-deficient mdx mice. *Neurobiol Learn Mem* **107**, 19-31, doi:10.1016/j.nlm.2013.10.017 (2014).

58 Lee, T. S. *et al.* Aquaporin-4 is increased in the sclerotic hippocampus in human temporal lobe epilepsy. *Acta Neuropathol* **108**, 493-502, doi:10.1007/s00401-004-0910-7 (2004).

59 Das, A. *et al.* Hippocampal tissue of patients with refractory temporal lobe epilepsy is associated with astrocyte activation, inflammation, and altered expression of channels and receptors. *Neuroscience* **220**, 237-246, doi:10.1016/j.neuroscience.2012.06.002 (2012).

60 Eid, T. *et al.* Loss of perivascular aquaporin 4 may underlie deficient water and K+ homeostasis in the human epileptogenic hippocampus. *Proc Natl Acad Sci U S A* **102**, 1193-1198, doi:10.1073/pnas.0409308102 (2005).

61 Medici, V., Frassoni, C., Tassi, L., Spreafico, R. & Garbelli, R. Aquaporin 4 expression in control and epileptic human cerebral cortex. *Brain Res* **1367**, 330-339, doi:10.1016/j.brainres.2010.10.005 (2011).

62 Kim, J. E. *et al.* Astroglial loss and edema formation in the rat piriform cortex and hippocampus following pilocarpine-induced status epilepticus. *J Comp Neurol* **518**, 4612-4628, doi:10.1002/cne.22482 (2010).

63 Sheen, S. H. *et al.* Decrease in dystrophin expression prior to disruption of brain-blood barrier within the rat piriform cortex following status epilepticus. *Brain Res* **1369**, 173-183, doi:10.1016/j.brainres.2010.10.080 (2011).

64 Taylor, P. J. *et al.* Dystrophin gene mutation location and the risk of cognitive impairment in Duchenne muscular dystrophy. *PLoS One* **5**, e8803, doi:10.1371/journal.pone.0008803 (2010).

639